Interaction between salinity intrusion and vegetation succession: A modeling approach

Su Yean Teh,[1, a)] Hock Lye Koh,[2, b)] Donald L. DeAngelis,[3, c)] and Mike Turtora[4, d)]
[1)] *School of Mathematical Sciences, Universiti Sains Malaysia, Penang 11800, Malaysia*
[2)] *UCSI University, No. 1, UCSI Heights, Jalan Menara Gading, Taman Connaught, Kuala Lumpur 56000, Federal Territory of Kuala Lumpur*
[3)] *U. S. Geological Survey and University of Miami, Coral Gables, Florida 33124, USA*
[4)] *U. S. Geological Survey, Gainesville, Florida 32605, USA*

(Received 27 March 2013; accepted 15 April 2013; published online 10 May 2013)

Abstract Predicting potential changes in groundwater salinity in low-lying coastal regions due to climate change is important, where coastal vegetation is abundant, succession competition between halophytes and glycophytes plays a significant role in the salinity budget. Sea level rise enhances salinity intrusion, contributing an additional dimension to vegetation competition. A new simulation model known as mangrove-hardwood hammock model coupled with saturated–unsaturated transport (MANTRA) has recently been developed by the authors to simulate groundwater salinity regimes in the presence of vegetation competition, subject to climate change. MANTRA is based upon linking two existing Unites States geological survey (USGS) simulation models known as mangrove-hardwood hammock model (MANHAM) and saturated–unsaturated transport (SUTRA). MANHAM simulates the evolution of vegetation succession subject to changing groundwater salinity. SUTRA simulates saturated and unsaturated transport of solutes and salinity in groundwater given sea salinity. MANTRA improves the simulation robustness to simultaneously simulate groundwater hydrology, salinity and coastal vegetation succession subject to sea level rise. Some simulation results will be presented to demonstrate the impact of sea level rise on coastal vegetation succession and groundwater salinity. [doi:10.1063/2.1303201]

Keywords salinity intrusion, groundwater, vegetation succession, MANTRA, climate change

I. INTRODUCTION

Climate change may bring about certain consequences to the environmental conditions and ecological systems in many parts of the world. It might alter patterns of precipitation, causing changes to the hydrological regimes. In low-lying coastal areas, the predicted sea level rise might alter groundwater salinity, inducing several associated alterations in coastal vegetation. The predicted climate change and its associated environmental alterations may affect biological process rates, leading to fundamental shifts in some coastal ecosystems. There have been some relevant studies suggesting potential shift in vegetation composition due to salinity disturbance. For example, the study by Baldwin and Mendelssohn[1] concluded that two adjoining plant communities, Spartina patens and Sagittaria lancifolia, might shift to a salt-tolerant or flood-tolerant species, depending on the level of flooding and salinity at the time of disturbance. Howard and Mendelssohn[2] in their study on the recovery ability of four species of marsh macrophytes from salinity pulses suggests that permanent shift in species composition may occur, depending on the severity of the short-term salinity pulses. Further, various literatures have highlighted the landward migration of mangroves as a result of sea level rise.[3–11] In this paper, we focus on simulating the impact of predicted sea level rise and associated changes in precipitation patterns on coastal groundwater (GW) hydrology and vegetation competition in low lying coastal regions and atolls, including south Florida coastal forests as discussed by Saha et al.[12] To predict coastal vegetation competition and succession between halophytes (salt tolerant) and glycophytes (salt intolerant), the authors have previously developed a simulation model known as mangrove-hardwood hammock model (MANHAM), which has been successfully used for simulating the competition between mangrove (halophyte) and hardwood hammock (glycophyte) in an environment of spatially and temporally varying groundwater salinity in southern Florida.[13,14] However, it is desirable to develop the capability of simultaneous simulation of vegetation competition and dynamically changing groundwater regimes over spatial-temporal scales. For this purpose, MANHAM must incorporate a dynamic sub-model for simulations of groundwater salinity. On the other hand, Unites States geological survey (USGS) has developed a suite of simulation models known as saturated–unsaturated transport (SUTRA) to simulate saturated–unsaturated transport of solutes in groundwater.[15–17] However, SUTRA does not have the capability to simulate vegetation competition. The newly developed MANHAM coupled with SUTRA (MANTRA) provides the capability to simultaneously simulate subsurface hydrological environment,

[a)] Corresponding author. Email: syteh@usm.my.
[b)] Email: hlkoh@usm.my.
[c)] Email: don_deangelis@usgs.gov.
[d)] Email: mturtora@usgs.gov.

Table 1. Groundwater use in some USA states.[18]

State	GW use intensity/ ($m^3 \cdot d^{-1} \cdot km^{-2}$)	Total GW use/ (10^6 $m^3 \cdot d^{-1}$)	Percentage of GW use to total water use
California	180	73	49
Hawaii	160	2.6	53
New Jersey	150	3	42
Florida	86	12	62
USA	—	310	39

and vegetation competition, subject to scenarios of climate change. We succeeded in dynamically linking MANHAM and SUTRA to allow robust simulations of vegetation competition when the groundwater itself is changing in elevation and salinity due to external forcing such as tides, tsunamis and other storm surges. In the following section, we provide a brief summary of groundwater hydrology relevant to this development.

II. CONCEPTS OF GROUNDWATER HYDROLOGY

A basic review of groundwater hydrology relevant to this paper is essential for linking SUTRA and MANHAM. Vast storage volumes of water are available under the ground for domestic, industrial and agricultural purposes if the water is not contaminated by pollutant or salt. Further, many streams and lakes are fed primarily or in large part by groundwater, indicating the importance of groundwater as an essential resource. Groundwater supplies almost 40% of non-saline water used in some USA states (Table 1). In particular, the state of Florida contains abundant groundwater resources, contributing 1.2×10^7 m^3/d of fresh groundwater, amounting to 62% of the entire water usage. Hence the importance of preserving and enhancing groundwater resources is beyond doubts.

Water infiltrates through the ground surface and percolates into the underlying strata, infiltrating first through an unsaturated zone *en route* to a saturated zone below. The water table separates the two unsaturated and saturated zones. The pressure at the water table is atmospheric. But there can be a capillary fringe to which water will rise above the water table. This capillary rise provides much of the soil moisture utilized by plants. In fine silty sands, the capillary rise can be as high as 50 cm, while the rise in gravel is only 2 to 3 cm. The water in this region fluctuates in quantity and quality depending on uptake by vegetation and percolation from infiltrated water. An aquifer is a water-bearing structure consisting of rocks and/or soils that can release its stored water in sufficient quantity to make it economically feasible to develop for water supply. The aquifer can be either confined or unconfined, depending on whether or not a water table or free water surface exists under atmospheric pressure. It is possible for a groundwater aquifer to become overlain by impermeable material and thus be under pressure, in which case it is known as a confined aquifer. Wells drilled into such confined aquifers are called artisan wells, which may provide free flowing water. Three parameters are of particular significance to this paper: (a) storage coefficient S (dimensionless) (b) hydraulic conductivity K (meter per day) and (c) hydraulic transmissivity T (meter square per day).

The storage coefficient S is defined as the volume of water that an aquifer releases or takes into storage per unit surface area of aquifer per unit change in head normal to that surface. For a vertical column of unit area extending through a confined aquifer, the storage coefficient S equals the volume of water released from the aquifer when the piezometric surface declines a unit distance. The storage coefficient is therefore a dimensionless quantity indicating a volume of water released per volume of aquifer. Typical values fall in the range $0.000\,05 \leqslant S \leqslant 0.005$, indicating that large pressure changes over extensive areas are required to produce substantial water yields. A rule of thumb relationship $S = 3 \times 10^{-6} \times b$ is often used to estimate S, where b is the saturated aquifer thickness in meters. Storage coefficient can best be estimated from pumping tests of wells or from groundwater fluctuation in response to atmospheric or ocean tide variations. Hydraulic conductivity K is defined as the volume of water (m^3) transmitted (at the prevailing kinematic viscosity) per unit time (d) per unit area of cross section (m^2) perpendicular to the direction of flow per unit of hydraulic gradient (dh/dL, dimensionless, where L (m) is the length of flow). The units are K = volume/(time·area) = $m \cdot d^{-1}$, indicating that hydraulic conductivity has the units of velocity $m \cdot d^{-1}$. Hydraulic conductivity K can vary significantly, depending on particle sizes (Table 2). Hydraulic transmissivity T is defined as the volume of water transmitted (at the prevailing kinematic viscosity) per unit time per unit width of aquifer per unit of hydraulic gradient. The units are T = volume/(time·width) = $m^2 \cdot d^{-1}$, indicating that hydraulic transmissivity T has the units of diffusion or dispersion $m^2 \cdot d^{-1}$. Note that $T = Kb$, where b is the saturated thickness of the aquifer. We nest present two simple analytical models to allow direct and quick interpretation of groundwater hydraulic responses subject to external tidal forcing.

III. ANALYTICAL MODEL FOR TIDAL INFLUENCE

A. Propagation of tidal signal

We first provide a simple mathematical description of changes in groundwater head h in response to tidal forcing in a confined aquifer. For simplicity, consider the one-directional flow in a confined aquifer as shown in Fig. 1. The differential equation governing the flow is

$$\frac{\partial^2 h}{\partial x^2} = \frac{S}{T} \frac{\partial h}{\partial t}, \tag{1}$$

Table 2. Values of hydraulic conductivity and particle size.[18]

Material	Hydraulic conductivity/ ($m \cdot d^{-1}$)	Particle size/ mm
Gravel, coarse	150	16.0–32.0
Gravel, medium	270	8.0–16.0
Gravel, fine	450	4.0–8.0
Sand, coarse	45	0.5–1.0
Sand, medium	12	0.25–0.5
Sand, fine	2.5	0.125–0.25
Silt	0.08	0.004–0.062
Clay	0.000 2	< 0.004

where h is the rise or fall of the piezometric surface with reference to the mean sea level, x is the distance inland from the outcrop, S is the storage coefficient of the aquifer, T is transmissivity and t is time. The amplitude of the tide is h_0 in meter (see Fig. 1). The appropriate boundary conditions are $h = h_0 \sin(\omega t)$ at $x = 0$ and $h = 0$ at $x = \infty$. The frequency ω is related to the tidal period t_0 by Eq. (2).

$$\omega = 2\pi/t_0. \tag{2}$$

The solution of Eq. (1) subject to the above boundary conditions is given by the formula

$$h = h_0 \exp[-x\sqrt{\pi S/(t_0 T)}] \cdot \sin\left[\frac{2\pi t}{t_0} - x\sqrt{\pi S/(t_0 T)}\right]. \tag{3}$$

From Eq. (3), it can be seen that the amplitude h_x of groundwater fluctuations at a distance x from the shore equals $h_x = h_0 \exp[-x\sqrt{\pi S/t_0 T}]$. The time lag t_{L} between the time series of ocean tide and the response of groundwater at the location x is given by the formula $t_{\mathrm{L}} = x\sqrt{t_0 S/(4\pi T)}$. This wave that propagates inland has a travelling velocity of $v_{\mathrm{w}} = x/t_{\mathrm{L}} = \sqrt{4\pi T/(t_0 S)}$ and a wavelength of $L_{\mathrm{w}} = v_{\mathrm{w}} t_0 = \sqrt{4\pi t_0 T/S}$. The amplitude decreases by a factor $\mathrm{e}^{-2\pi}$ for each wavelength. Water flows into the aquifer during half of each cycle and flows out during the other half with a volume given by $V = h_0\sqrt{2t_0 ST/\pi}$. The above analysis is also applicable to a good approximation to water table fluctuations of an unconfined aquifer if the range of fluctuations is small in comparison to the saturated thickness. The simple analytical formulation provides a basis for the estimation of aquifer parameters such as hydraulic transmissivity T.

B. Fresh water lens thickness

We consider a circular island of radius R (Fig. 2) receiving an effective recharge from rainfall at a rate

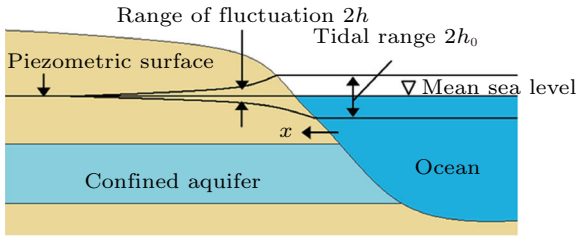

Fig. 1. Groundwater level fluctuations produced by ocean tides in a confined aquifer.

W. The outward flow Q at location with radius r is given by

$$Q = 2\pi r K (z + h)\frac{\mathrm{d}h}{\mathrm{d}r}, \tag{4}$$

where K is the hydraulic conductivity and h and z are defined in Fig. 2. Noting $h = (\Delta\rho/\rho)\, z$, with ρ the density of sea water, and $Q = \pi r^2 W$, we have

$$z\mathrm{d}z = \frac{W r \mathrm{d}r}{2K(1 + \Delta\rho/\rho)(\Delta\rho/\rho)}. \tag{5}$$

Integrating and applying the boundary condition of $h = 0$ when $r = R$, we obtain

$$z^2 = \frac{W(R^2 - r^2)}{2K(1 + \Delta\rho/\rho)(\Delta\rho/\rho)}. \tag{6}$$

Thus, the depth z to salt water at any location x is a function of the rainfall recharge W, the size of the island R and the hydraulic conductivity K. The thickness of the fresh water lens is given by z_0, obtained by substituting $r = 0$ in Eq. (6). It is clear from Eq. (6) that the fresh water lens thickness is directly proportional to the radius R of the circular island. In the scenario of sea level rise, a small increase in sea level may produce a significant reduction in the value of R for low lying atolls with mild slope. The implication is that the fresh water lens may be significantly reduced in its thickness. This significant reduction in fresh water lens dimension poses severe threat to the livelihood of the residents in low lying atolls.

IV. MANHAM + SUTRA = MANTRA

Sea level rise associated with global climate change will increase the threat posed by storm surges to coastlines and islands. Further, tropical storms and mega tsunami may inundate many coastal regions with large volumes of highly saline sea water. There is a need to understand and predict the consequences of a storm surge or a series of storm surges on both the short-term dynamics of salinity in the soil and groundwater of an inundated area and the long-term ecological effects. The long-term effects will be determined not only by

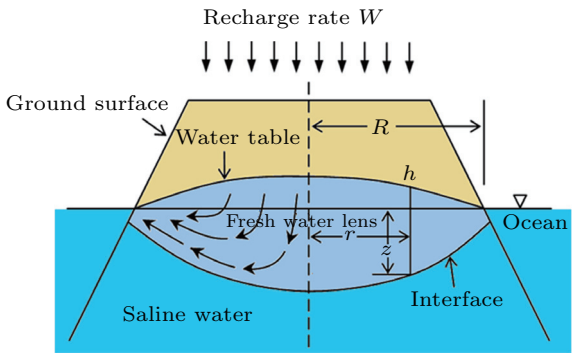

Fig. 2. Fresh water lens in an oceanic island under natural conditions.

the magnitude of the overwash, but also by the subsequent interactions between groundwater, tides, precipitation, and vegetation dynamics. Our overarching scientific objective is to develop a quantitative understanding on the potential consequences of climate change on the availability and quality of water resources and the subsequent vegetation distribution in space and time in low lying coastal areas, with a particular focus on atoll islands. For this purpose, USGS has developed two simulation models namely MANHAM and SUTRA. MANHAM is a simulation model for predicting the long term evolution of coastal vegetation subject to inter and intra species competition in an environment of changing salinity. In MANHAM, the biomasses of mangrove and hardwood hammock are explicitly modeled with the plants differing in their ability to compete for light and tolerances for salinity. Within each computational cell, the vegetations interact both by shading of light and altering the common salinity of the vadose zone. The biomasses for hardwood hammock and mangrove at a computational cell depend on the gross productivity, respiration and litterfall of each plant. The mathematical equations used in MANHAM to describe the competition between hardwood hammock and mangrove are available in Refs. 13 and 14. The salinity of the soil (vadose zone) in each spatial cell is determined by the difference between the precipitation, which brings in fresh water, and the evaporation, and plant uptake of water. The uptake of water (respiration) by the hardwood hammock and mangrove species is given by the empirical relations as a function of salinity. The MANHAM model simulates the vadose or unsaturated zone of the soil. It models movement of water and salinity in the vadose zone, as influenced by precipitation, tides, evaporation, evapotranspiration of vegetation, and movement of water upwards from the groundwater. It also simulates the dynamics of the vegetation, including that of competing vegetation types with different salinity tolerance. However, it does not model the dynamics of the groundwater underlying the vadose zone, which, in coastal areas and atolls, typically consists of a fresh water lens on top of deeper water with salinity levels close to the neighboring sea water. This fresh water lens constitutes an important component of the water balance for the overlying vegetation through transpiration and plays a key role on the salinity balance as well, which has not been considered in the existing model formulations of MANHAM. MANHAM assumes that the groundwater is a constant boundary condition. This assumption of boundary constancy is certainly violated on small atoll islands, in which tides cause diurnal fluctuations in groundwater, as may be seen from the discussion in the previous section. Further, tsunami and storm surges can cause major changes to groundwater salinity that can last for years. SUTRA, on the other hand, simulates variable-density groundwater flow, and quantifies the hydraulic and salinity gradients in the freshwater–saltwater transition zone associated with the fresh water lens according to the following partial differential equation (7). This equation is solved numerically by the finite element method

$$\left(S_{\mathrm{w}}\rho S_{\mathrm{op}} + \varepsilon\frac{\partial S_{\mathrm{w}}}{\partial p}\right)\frac{\partial p}{\partial t} + \left(\varepsilon S_{\mathrm{w}}\frac{\partial p}{\partial U}\right)\frac{\partial U}{\partial t} - \nabla\cdot\left[\left(\frac{kk_{\mathrm{r}}}{\mu}\right)\cdot(\nabla p - \rho g)\right] = Q_{\mathrm{p}}. \tag{7}$$

SUTRA has been successfully used to simulate salinity intrusion due to tidal effects in unconfined aquifers,[19] in salt marshes,[20,21] in barrier islands due to overwash[22] as well as in coastal region in India arising from human activities.[23] Three-dimensional version of SUTRA has also been applied on a coastal aquifer in southern Oahu, Hawaii, USA.[24] Therefore, the success in linking MANHAM and SUTRA provides a new suite of simulation models known as MANTRA to improve the calculation of vegetation-water-salinity interactions on atoll islands, as well as other low-lying islands and coastal areas.[25] However, this initial success requires continuing improvement to obtain a robust and better forecast of the short- and long-term effects of overwash events that may result from tsunami or storm surge on a low-lying island or atoll, and refine our hypothesis that a regime shift may occur. This MANTRA model will be driven by both existing climate observations and projections of climate change scenarios (Fig. 3). Another specific objective is to develop and apply remote sensing methods for tracking possible vegetation regime changes on atolls, small islands, and coastal areas, and for the calibration and validation of MANTRA simulation models, as well as for testing of our hypothesis regarding potential short- and long-term vegetation shifts due to climate change. Vegetation shift can pose serious threat, both to groundwater supply as well as food crops.

V. APPLICATION OF MANTRA

MANTRA is designed for application to low-lying coastal areas and atoll islands. Sea level rise (SLR) is one of the most significant predicted consequences of global climate change and has the potential for severe effects on the vegetation of low-lying coastal areas, islands and atoll islands.[26] Rising sea level would also

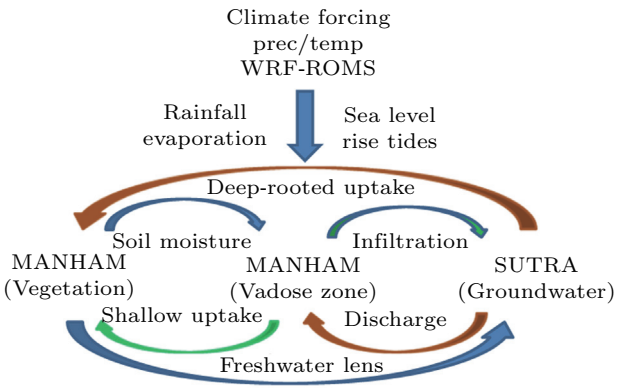

Fig. 3. Linkage of the MANHAM model modules of vegetation and vadose zone hydrology and salinity with the SUTRA model of groundwater hydrology and salinity, driven by dynamically downscaled climate variables.

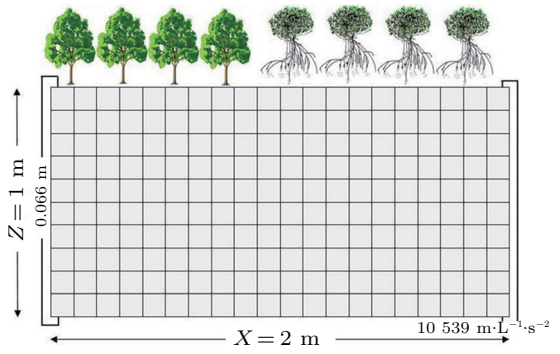

Fig. 4. MANHAM–SUTRA computational domain consisting of a cross section of 2 m horizontal width and 1 m vertical depth.

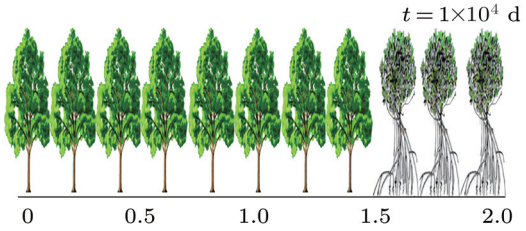

Fig. 5. Distribution of hardwood hammock and mangrove biomass after 27 years of simulation.

mean higher storm surges, and potential increase in the intensity and frequency of the storm surges. A calculation made by Ref. 27 indicates that the current 100-year flood levels will occur 3 to 4 times more frequently by the end of the 21st century in the mid-Atlantic coastal region. The impact of mean SLR will be a gradual shoreline retreat and subsequent loss of ecosystem area in these locations. However, large scale ocean water intrusion through storm surges may affect large areas on a short time scale, including the inundation of whole low-lying atolls. The immediate effect will be on the fresh water lenses that sit on top of saline groundwater in these areas (see Fig. 2). Such effects on available fresh water may have negative consequences for the populations of coastal areas and, particularly, atoll islands, as they depend critically on fresh water stored in the lenses.[28] In addition to the effects on water quality, a less obvious effect of SLR and the expected overwash events could be the short- and long-term effects on vegetation. Stable boundaries are often maintained between halophytic and glycophytic vegetation by self-reinforcing feedbacks, as each type of vegetation, once established, tends to create vadose zone salinity conditions that favor itself. If a large disturbance in soil salinity overwhelms these feedbacks, even for a short period of time, the boundaries may no longer be maintained; that is, a type of regime shift can occur. Large areas of fresh water vegetation may be replaced by halophytic vegetation following tsunami or storm surge overwash, which may lead to permanent salinization of the vadose zone.

VI. MANTRA SIMULATION RESULTS

This section provides simulation results for analyzing the competition between a halophyte and a glycophyte in an environment of changing salinity due to climate change by means of MANTRA. Climate change may induce changes to precipitations and sea level. For the sake of clarity and simplicity, a habitat consisting of a line of length 2 m perpendicular to the coast is chosen (Fig. 4). This may be thought of as a vertical line section cutting across a uniform domain of infinite width. This habitat is then superimposed onto a 2-D vertical cross section consisting of a vertical rectangle of width 2 m and depth 1 m. This choice may seem to be arbitrary, but is intended as a proof of capability. The scaling up and other remaining details is straightforward and can be sorted out later. The computational domain is discretized into 200 square finite elements of dimension 0.1 m × 0.1 m. For clarity, we denote by X the horizontal dimension and Z the vertical dimension. We assume that the lens has a horizontal thickness of 1 m in the Y-direction. We assume further that there is a constant flux of fresh water from the left boundary at the total rate of 0.066 kg/d evenly distributed along the 11 boundary nodes. The right boundary is exposed to a sea water intrusion with a salinity of 3.57%. The simulation begins with fresh water in all computational nodes except at the right sea boundary. Initial random distribution of hardwood hammock and mangrove biomass is employed in this simulation. The simulation is run for 1×10^4 d (about 27 years) with a time step of $\Delta t = 1$ d.

A. Hypothetical scenario 1

Under hypothetical scenario 1, we assume that the rate of fresh water inflow from the left land boundary

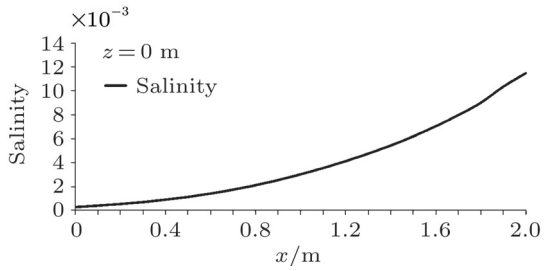

Fig. 6. Salinity profile in the X-direction at $z = 0$ m after 27 years of simulation.

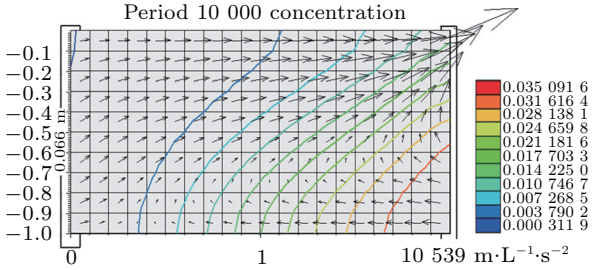

Fig. 7. Computational domain showing the finite elements, flow velocity and salinity contours.

is 0.066 kg/d and that the sea salinity on the right boundary is 3.57%. Figure 5 shows the final distribution of hardwood hammock and mangrove biomass after 27 years of simulation, indicating the dominance of mangrove biomass in the region with high salinity (near to the coast). On the other hand, the dominance of hardwood hammock biomass in the region with low salinity (fresh water input) is indicated. The distribution of salinity at the surface $Z = 0$ m is demonstrated in Fig. 6, indicating a maximum salinity of 1.2% at the seaward boundary node. The salinity at the seaward boundary nodes increases with depth due to increasing salinity flux with depth, as should be expected from theory. Figure 7 demonstrates the computational domain showing the finite elements, flow velocity and salinity contours. At the bottom of the simulated aquifer, salt water intrusion dominates the fresh water inflow, pushing the salinity profile landward. On the other hand, on

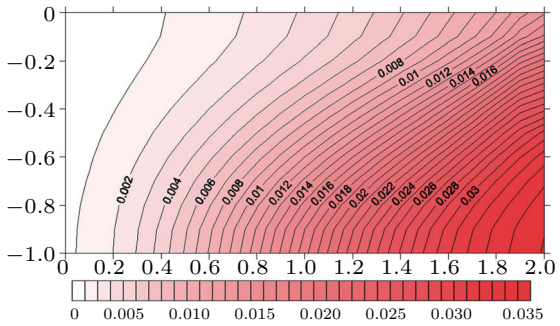

Fig. 8. Salinity contours after 27 years of simulation.

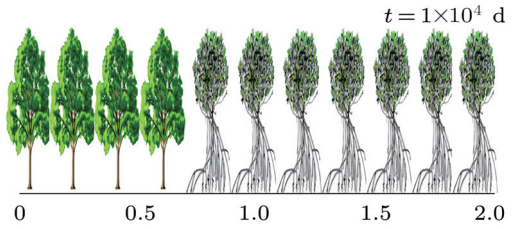

Fig. 9. Distribution of hardwood hammock and mangrove biomass after 27 years of simulation with 50% reduction in fresh water inflow, showing landward migration of mangrove biomass due to increased salinity.

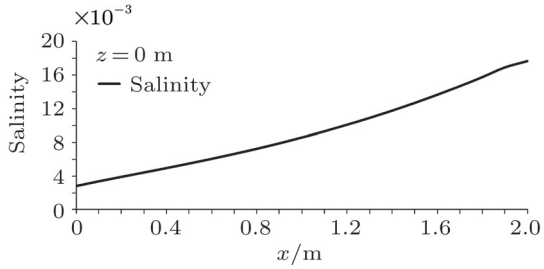

Fig. 10. Salinity profile in the X-direction at $Z = 0$ m after 27 years of simulation with 50% reduction in fresh water inflow.

top of the simulated aquifer, the lower hydrostatic pressure allows the fresh water flow to dominate, resulting in the salinity contour being pushed seaward. There is a net inflow of fresh water into the aquifer, resulting in a net flow at the top of the seaward boundary. Figure 8 shows the salinity contours simulated after 27 years.

B. Hypothetical scenario 2

For the hypothetical scenario 2, we assume that the fresh water flow is reduced by 50%, due in part to climate change, while maintaining the sea level as before. Figure 9 shows the impact of a 50% reduction in fresh water inflow on the distribution of hardwood hammock and mangrove biomass, showing landward migration of

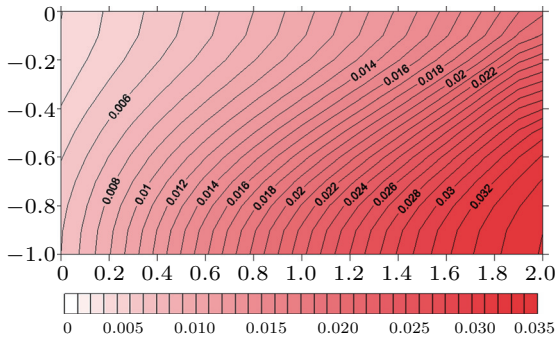

Fig. 11. Salinity contours after 27 years of simulation with 50% reduction in fresh water inflow.

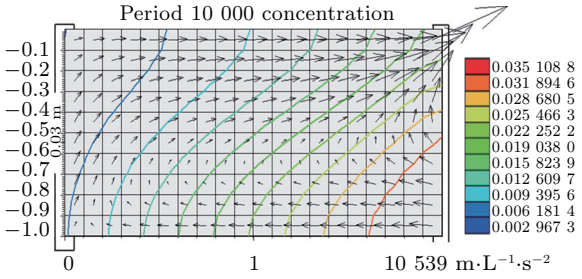

Fig. 12. Computational domain showing the finite elements, flow velocity and salinity contours with 50% reduction in fresh water inflow.

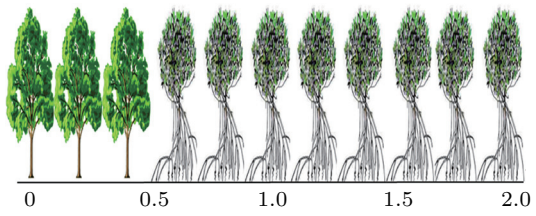

Fig. 13. Final distribution of hardwood hammock and mangrove biomass after 27 years of simulation, hypothetical scenario 3.

mangrove biomass due to increased salinity. The increase in salinity due to a 50% reduction in fresh water inflow is clearly demonstrated in Figs. 10–12. The zone of convergence between fresh water and salt water has been moved further inland due to a 50% reduction in fresh water input. The landward intrusion of saline water can pose serious threats to population living along low-lying coasts.

C. Hypothetical scenario 3

For the hypothetical scenario 3, we assume that the fresh water flow is maintained as in hypothetical scenario 1 but the sea level is increased due to sea level rise so that the pressure at each of the seaward nodes is increased by 30%, according to the formulation of MANTRA. Figure 13 shows the impact of sea level rise on the distribution of hardwood hammock and mangrove biomass, showing landward migration of mangrove biomass due to increased salinity. The increase in salinity due to this sea level rise is clearly demonstrated in Figs. 14–16. The zone of convergence between salt water and fresh water has been moved further inland due to this sea level rise. This landward intrusion of saline water poses threat to water resources along atolls and low-lying coastal areas.

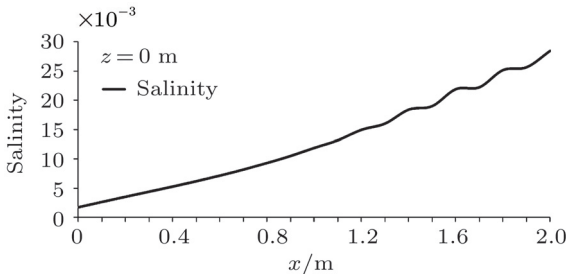

Fig. 14. Salinity profile in the X-direction at $Z = 0$ m after 27 years of simulation, hypothetical scenario 3.

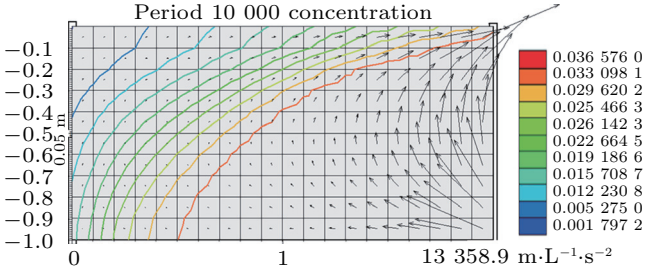

Fig. 15. Computational domain showing the finite elements, flow velocity and salinity contours, hypothetical scenario 3.

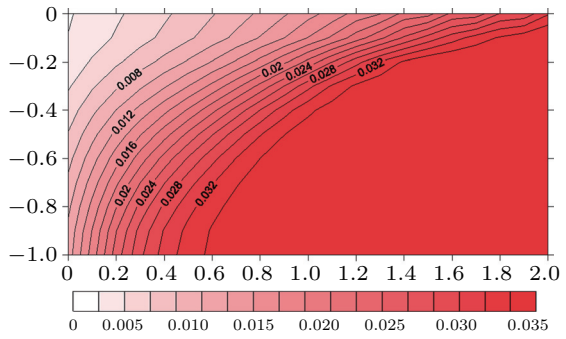

Fig. 16. Salinity contours after 27 years of simulation hypothetical scenario 3.

VII. CONCLUSION

This paper has presented the development of a new suite of simulation models known as MANTRA to simulate the impact of sea level rise on salinity intrusion, on groundwater hydrology and on their associated impact on vegetation shift. Three simulations have been conducted on hypothetical scenarios of climate change resulting in altered precipitation patterns and sea level rise. There is a need to further enhance the robustness of MANTRA as well as to improve on-site data regarding sub-surface hydrology and vegetation ecosystem to allow improved simulations. We plan to also use remote sensing techniques to improve on-site data collection, which will be pursued in the near future under the sponsorship of USGS grant.

This work was supported by (1001/PMATHS/811093, 1001/PMATHS/821045). The first two authors would like to express our appreciation to USGS and the University of Miami for providing financial grants to permit travel to Miami to complete this research.

1. A. H. Baldwin, and I. A. Mendelssohn, Aquatic Botany **61**, 255 (1998).
2. R. J. Howard, and I. A. Mendelssohn, American Journal of Botany **86**, 795 (1998).
3. J. C. Ellison, and D. R. Stoddart, Journal of Coastal Research **7**, 151 (1991).
4. J. C. Ellison, Estuarine Coastal and Shelf Science **37**, 75 (1993).
5. C. D. Field, Hydrobiologia **295**, 75 (1995).
6. R. Lara, C. Szlafsztein, and M. Cohen, et al., Journal of Coastal Conservation **8**, 97 (2002).
7. T. W. Doyle, G. F. Girod, and M. A. Books, *Modeling mangrove forest mitigation along the southwest coast of Florida under climate change*, edited by Z. H. Ning et al. (GCRCC and LSU Graphic Services, Baton Rouge, 2003) 211.
8. E. McLeod, and R. V. Salm, *Managing Mangroves for Resilience to Climate Change* (The World Conservation Union (IUCN), Gland, 2006).
9. E. L. Gilman, J. Ellison, and N. C. Duke, et al., Aquatic Botany **89**, 237 (2008).
10. M. C. França, M. I. Francisquini, and M. C. L. Cohen, et al., Review of Palaeobotany and Palynology **187**, 50 (2012).
11. S. C. Yang, S. S. Shih, and G. W. Hwang, et al., Ecological Engineering **51**, 59 (2013).
12. A. K. Saha, S. Saha, and J. Sadle, et al., Climatic Change **107**, 81 (2011).
13. L. Sternberg, S. Y. Teh, and S. Ewe, et al., Ecosystems **10**, 648 (2007).
14. S. Y. Teh, D. L. DeAngelis, and L. S. L. Sternberg, et al., Ecological Modelling **213**, 245 (2008).
15. C. I. Voss, *SUTRA: A finite-element simulation model for saturated–unsaturated, fluid density-dependent groundwater flow with energy transport or chemically-reactive single species solute transport*. U. S. Geological Survey, Water Resources Investigations Report, 1984-4369 (1984).
16. C. I. Voss, *USGS SUTRA code — History, practical use, and application in Hawaii*. Pages 249–313, edited by J. Bear, A. H.D. Cheng, and S. Sorek, et al. (Kluwer Academic Publishers, The Netherlands, 1999) 249.
17. C. I. Voss, and A. M. Provost, *A model for saturated–unsaturated, variable-density ground-water flow with solute or energy transport*. U. S. Geological Survey, Water Resources Invest. Report 2002-4231 (2002).
18. D. K. Todd, and L. W. Mays, *Groundwater Hydrology*, Third Edition. (John Wiley & Sons, Inc., New York, 2005)
19. B. Ataie-Ashtiani, R. E. Volker, and D. A. Lockington, Journal of Hydrology **216**, 17 (1999).
20. A. M. Wilson, and L. R. Gardner, Water Resources Research **42**, W01405 (2006).
21. E. S. Carter, S. M. White, and A. M. Wilson, Estuarine, Coastal and Shelf Science **76**, 543 (2008).
22. W. P. Jr. Anderson, and R. M. Lauer, Hydrogeology Journal **16**, 1483 (2008).
23. A. G. Bobba, Hydrological Sciences Journal **47**, S67 (2002).
24. S. B. Gingerich, and C. I. Voss, Hydrogeology Journal **13**, 436 (2005).
25. S. Y. Teh, H. L. Koh, and D. L. DeAngelis, et al., Hydogeology Journal **18**, 749 (2011).
26. R. J. Nicholls, and A. Cazenave, Science **328**, 1517 (2010).
27. R. G. Najjar, H. A. Walker, and P. J. Anderson, et al., Climate Research **14**, 219 (2000).
28. W. P. Jr. Anderson, Journal of Coastal Research **18**, 413 (2002).